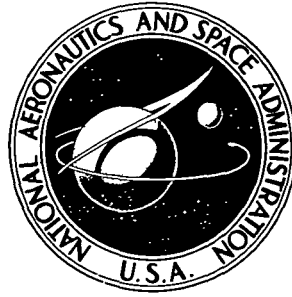


NASA TECHNICAL NOTE



NASA TN D-8500

NASA TN D-8500

**RESULTS OF ANALYSES PERFORMED
ON SOIL ADJACENT TO PENETRATORS
EMPLACED INTO SEDIMENTS AT
McCOOK, NEBRASKA, JANUARY 1976**

*M. Blanchard, T. Bunch, A. Davis, F. Kyte,
H. Shade, J. Erlichman, and G. Polkowski*

*Ames Research Center
Moffett Field, Calif. 94035*

1 Report No NASA TN D-8500		2 Government Accession No		3 Recipient's Catalog No	
4 Title and Subtitle RESULTS OF ANALYSES PERFORMED ON SOIL ADJACENT TO PENETRATORS EMPLACED INTO SEDIMENTS AT McCOOK, NEBRASKA, JANUARY 1976				5 Report Date July 1977	
				6 Performing Organization Code	
7 Author(s) M Blanchard,* T Bunch,* A Davis,** F Kyte ** H Shade*** J Erlichman,*** and G Polkowski***				8 Performing Organization Report No A-6907	
9 Performing Organization Name and Address *NASA-Ames Research Center, Moffett Field, Calif 94035 **San Jose State University, San Jose, Calif 95192 ***L F E Corp, Richmond, Calif 94804				10 Work Unit No 186-68-76-06	
				11 Contract or Grant No	
12 Sponsoring Agency Name and Address National Aeronautics and Space Administration Washington, D C 20546				13 Type of Report and Period Covered Technical Note	
				14 Sponsoring Agency Code	
15 Supplementary Notes					
16 Abstract During 1976 several penetrators (full and 0 58 scale) were dropped into a test site at McCook, Nebraska. The McCook site was selected because it simulated penetration into wind-deposited sediments (silts and sands) on Martian plains. This report describes the physical and chemical modifications found in the sediment after the penetrators' impact. Laboratory analyses have shown mineralogical and elemental changes are produced in the sediment next to the penetrator. Optical microscopy studies of material next to the skin of the penetrator revealed a layer of glassy material about 75 μ m thick. Elemental analysis of a 0-1-mm layer of sediment next to the penetrator revealed increased concentrations for Cr, Fe, Ni, Mo, and Na, and reduced concentrations for Mg, Al, Si, P, K, and Ca. The Cr, Fe, Ni, and Mo were in fragments abraded from the penetrator. Mineralogical changes occurring in the sediment next to the penetrator include the introduction of micron-size grains of α iron and several hydrated iron oxide minerals. The newly formed silicate minerals include metastable phases of silica (cristobalite, lechatelierite, and opal). The glassy material was mostly opal which formed when the host minerals (mica, calcite, and clay) decomposed. In summary, contaminants introduced by the penetrator occur up to 2 mm away from the penetrator's skin. Although volatile elements do migrate and new minerals are formed during the destruction of host minerals in the sediment, no changes were observed beyond the 2-mm distance. The analyses indicate 0 58-scale penetrators do effectively simulate full-scale testing for soil modification effects.					
17 Key Words (Suggested by Author(s)) Penetrators Mars exploration Planetary missions				18 Distribution Statement Unlimited STAR Category 91	
19 Security Classif (of this report) Unclassified		20 Security Classif (of this page) Unclassified		21 No of Pages 29	
				22 Price* \$3.25	

RESULTS OF ANALYSES PERFORMED ON SOIL ADJACENT TO PENETRATORS

EMPLACED INTO SEDIMENTS AT McCOOK, NEBRASKA, JANUARY 1976

M. Blanchard,* T. Bunch,* A. Davis,** F. Kyte,** H. Shade,*** J. Erlichman,***
and G. Polkowski***

SUMMARY

During 1976 several penetrators (full and 0.58 scale) were dropped into a test site at McCook, Nebraska. The McCook site was selected because it simulated penetration into wind-deposited sediments (silts and sands) on Martian plains. This report describes the physical and chemical modifications found in the sediment after the penetrators' impact.

Laboratory analyses have shown mineralogical and elemental changes are produced in the sediment next to the penetrator. Optical microscopy studies of material next to the skin of the penetrator revealed a layer of glassy material about 75 μm thick. Elemental analysis of a 0–1-mm layer of sediment next to the penetrator revealed increased concentrations for Cr, Fe, Ni, Mo, and Na, and reduced concentrations for Mg, Al, Si, P, K, and Ca. The Cr, Fe, Ni, and Mo were in fragments abraded from the penetrator. Mineralogical changes occurring in the sediment next to the penetrator include the introduction of micron-size grains of α iron and several hydrated iron oxide minerals. The newly formed silicate minerals include metastable phases of silica (cristobalite, lechatelierite, and opal). The glassy material was mostly opal which formed when the host minerals (mica, calcite, and clay) decomposed.

In summary, contaminants introduced by the penetrator occur up to 2 mm away from the penetrator's skin. Although volatile elements do migrate and new minerals are formed during the destruction of host minerals in the sediment, no changes were observed beyond the 2-mm distance. The analyses indicate 0.58-scale penetrators do effectively simulate full-scale testing for soil modification effects.

INTRODUCTION

During fiscal year 1976, a field-test program (ref 1) was conducted at terrestrial analog sites selected to represent anticipated Martian materials in which the penetrator would experience maximum and minimum penetration depths. Maximum penetration occurred at McCook, Nebraska. The McCook site was selected because it simulated penetration into wind-deposited sediments (silts and sands) on Martian plains.

*Ames Research Center

**San Jose State University

***L. F. E. Corp

This report describes the following features for the McCook field tests (1) the physical and chemical alteration of the soil caused by the impacting penetrator, (2) the amount of contamination introduced to the soil by the penetrator during impact, and (3) the effectiveness of 0.58 scale penetrators to reproduce soil alteration and contamination identical to full-scale penetrators.

Several earlier reports (refs. 2 and 3) reported results of preliminary studies performed on uncontrolled penetrator tests in sediments. The McCook site was deemed suitable based on mineralogical analyses of core samples (ref. 4) and procedures developed to preserve sedimentary fabric around penetrators (ref. 5).

The authors acknowledge the suggestions rendered by T. Canning, R. Jackson, and R. Reynolds at Ames and thank R. Clayton at Ames for the excellent photomicrography. Some preliminary analysis were performed by E. Reece and G. Nelson of Sandia Corporation. The success of our analysis was in large part dependent on the recovery methods conceived by P. Gerhart and F. Purdy, Woodward and Clyde, Denver, Colorado, and employed in McCook, Nebraska, for retrieving the penetrators in-situ and surrounding soil column. Quantitative X-ray fluorescence analysis was conducted by G. Cunningham, University of Oregon, Eugene. Motivation for the initial effort was provided by Dr. W. Quaide, past Planetary Science and Applications Branch Chief (now at NASA Headquarters). Finally, we had many helpful discussions with Dr. J. Fruchter, Battelle-Pacific Northwest Laboratories, Richland, Washington, geochemist on the Ad Hoc Surface Penetrator Science Committee chaired by Dr. J. Westphal, California Institute of Technology.

PROCEDURES

The field-test procedures involved dropping two full-scale penetrators from a fixed-wing aircraft (fig. 1) at altitudes above 1500 m to achieve an impact velocity of ~ 130 m/sec, and two 0.58-scale penetrators from a trailer-mounted airgun (fig. 2) at slightly higher impact velocities. The full-scale penetrators landed in sites having two different types of sediments: loess, and layered silts and clays. The 0.58-scale penetrators were fired into these same sediments within a few feet of the full-scale units. One set (full scale and 0.58 scale) of penetrators landed in a true loess sediment (fig. 3) and the other set landed in a layered clay and silt sediment. Penetration depths (table 1) for all tests were less than anticipated because the top 30 cm of the ground was frozen. Because the field tests were performed during the winter, Woodward and Clyde Laboratories developed a recovery method to retrieve the penetrator and surrounding soil column intact. With this method, a large-diameter hole (162-cm diam) was drilled down to the aft end of the buried penetrator. Then eight smaller holes (about 46-cm diam) were drilled (fig. 4(a)) to a depth equal to the penetrator's length just inside the walls of the larger hole. This process left a remaining pedestal of soil (about 70-cm diam and 122-cm height) containing the penetrator forebody (fig. 4(b)). This remaining column was carved into a cylindrical shape by use of a cutting bar with a jig and wall braces (fig. 5), wrapped in plastic, covered with polyurethane foam, and encased in a stainless-steel container. The container, when closed, kept the soil column under compression to prevent disturbance of the soil structures during transportation. The containers were taken to a Woodward and Clyde soil laboratory (fig. 6) in Denver, Colorado, where soil samples were recovered.

Sample recovery included opening the containers and removing the sediment in layers to reach the penetrator. Soil samples adjacent to each penetrator were removed with spatulas and sealed in

small containers (fig. 7). These samples were removed in layers at successively closer distances to the skin of the penetrator 1 cm, 2 mm, 1 mm, and coating on penetrator skin. These layers were taken from the nose to the aft end of each penetrator in 10-cm sections. Also, undisturbed samples of soil were recovered for comparison.

During this activity, all features showing deformation caused by the penetrator during impact were studied and photographed. Also, soil moisture levels were measured on samples taken both before encasement (at McCook) and during soil sampling (at Denver) two weeks later.

Analytical studies performed on the skin of the penetrator and the surrounding soil samples included: optical microscopy, scanning electron microscopy, electron microprobe, X-ray diffraction, and X-ray fluorescence

RESULTS

The moisture content in the soil during encasement and transportation remained essentially unchanged. The moisture content just before encasement (table 1) was between 15 to 16-percent dry weight for the four impact sites. The moisture content in the soil during recovery at the Woodward and Clyde Laboratories was between 14 to 17-percent dry weight. Measurements taken on undisturbed samples indicate the soil saturates at about 22-percent soil moisture. Because of the relatively large amounts of moisture present in the soil, the metal abraded from the penetrator alloy could be expected to rust soon after emplacement.

Observations indicate that the original sedimentary structures were modified by the impact of the penetrator. The clay and silt layers in the sediment were deformed (fig 8) as the penetrator passed through them. Drag folds developed about 5 cm from the penetrator, rotating some of the once horizontal layers to a vertical orientation about 1 cm from the penetrator. In this zone (0–1 cm), the sediment was mixed and crushed so that nearly all evidence of the original layers was destroyed. A series of parallel shear planes (fig. 9) now characterize the only structure evident in this zone. These shear planes can be approximately described as a series of echelon conical-shaped surfaces having their apex pointing toward the penetrator's nose and intersecting the penetrator's skin at 5–10° angles.

Analyses were performed on the soil layers immediately adjacent to each penetrator. Size distribution studies that compare the undisturbed with the modified sediment for the two full-scale penetrators show a significant increase in the particulate material greater than 125 μm and a corresponding reduction for particulate material smaller than 8 μm . These changes, occurring in the modified sediment adjacent to the skin of the penetrators, suggest a glassy material (similar to the glass produced when drilling in sedimentary rocks, as reported in ref. 6) was formed at the expense of the clay size ($< 8 \mu\text{m}$ in fig. 10) mineral constituents. Similar changes were observed when the undisturbed and modified sediments surrounding the two 0.58-scale penetrators were examined.

Optical microscopy studies of the material next to the skin from both full-scale and 0.58-scale penetrators revealed a layer of dark brown glassy material. A layer, opaque to transmitted light in thin section, next to the skin was 10–75 μm thick. Farther away from the skin, the original mineral

grains were visible but were surrounded by a translucent brown matrix (fig. 11). This colored matrix disappears approximately 2 mm away from the penetrator's skin. This matrix has sufficient strength to hold the soil particles together in cohesive pieces as large as 1 cm X 1 cm and up to 2 mm thick (fig. 12). This cohesiveness is typical for soil from both the full-scale and 0.58-scale penetrators and suggests that the soil particles have been sintered. Striations prominently mark the face of the glassy material (fig. 13). These striations are impressions made by the machine marks remaining on the penetrator's surface. Occasionally, another set of striations occurs perpendicular to the first set. This second set is parallel with the direction of forward motion of the penetrator and appears to be casts of grooves produced when material abraded from the penetrator's skin as it moved through the soil.

A profile analysis (fig. 14) was performed with the electron microprobe across the glassy material, the sintered matrix, and the adhering sediment to measure the Fe and Cr distribution in a soil sample from penetrator 4. The Fe content ranged from 1 to 54 percent. Two trends were evident for the Fe content. One trend, shown by a variable Fe content ranging from 10 to 30 percent and gradually decreasing away from the penetrator, was caused by metal abraded from the penetrator and introduced into the host sediment. The other trend, shown by a consistently lower Fe content of 1 to 2 percent clearly discernible as the profile moved away from the penetrator, represented the natural Fe abundance in the original sediments. The Cr content was about 3 percent in the glassy material and rapidly dropped to the ppm level within 1 mm of the penetrator's skin. The concentration of Cr, Ni, and Mo was greater at the surface of the glassy material (fig. 15) than it was in the D6AC alloy (table 2).

Comparison of bulk elemental composition between undisturbed and modified sediment adjacent to penetrator 4 showed changes for most elements (table 3). The surface of the glassy material was enriched significantly in Cr (up to 12.5 percent), Fe (up to 49.0 percent), Ni (up to 0.17 percent), and Mo (up to 7.4 percent), and perhaps Ca (up to 6.2 percent). All other elements were depleted, especially Na (down to 0.03 percent) and Si (down to 2.4 percent). Bulk analysis of sediment in the 0–1-mm layer (includes glassy material) revealed increased concentrations for Cr, Fe, Ni, Mo, and Na and reduced concentrations for Mg, Al, Si, P, K, and Ca. Bulk analysis on soil samples from the 0–1-mm glassy zone for penetrators 2, 3, and 5 also showed Cr, Fe, Ni, and Mo at significantly increased levels (table 4). Also, Na, Al, Si, and K were always depleted. Bulk analysis of sediment in the 1–2-mm layer still showed concentrations of Cr, Fe, Ni, and Na above their natural level in the undisturbed sediments. Usually, Na was depleted in the glassy material and then became enriched, relative to undisturbed sediments, 1 to 2 mm away from the penetrator's skin. In contrast, Ca was sometimes depleted and sometimes enriched in the glassy material. In most cases, the concentration of Cr, Fe, Ni, and Mo returned to their natural level in the undisturbed sediments about 2 mm from the penetrator.

The mineralogical changes occurring in the sediments next to the penetrator include both the introduction of new material and the formation of new phases (table 5) in three zones. (1) Within the glassy material, micron-sized grains of α iron were introduced along with abundant hydrated iron oxide minerals (i.e., goethite, lepidocrocite, ϵ Fe_2O_3 , and limonite). Also, a few grains of a Cu-Sn alloy were found. The new silicate minerals identified included cristobalite, lechatelierite, and opal. The glassy material was mostly opal. Conspicuously absent from the sediment in this zone were mica, clay, and calcite minerals from the host sediment. (2) Within the 0–1-mm zone of modified sediment, again micron-sized grains of α iron were introduced along with several newly formed hydrated iron oxides. A single grain of a Cu-Sn alloy was found. This Cu-Sn alloy particle was a fragment abraded from the screws that sheared off when the afterbody separated from the

forebody during impact with the ground surface. The one newly formed silicate mineral was opal, but it was not as abundant as in the glassy layer. Nearly all of the minerals in the host sediment were found in this zone. The identification of calcite is uncertain, but, if present, it would occur only in trace quantities. (3) Within the 1–2-mm zone of modified sediments, again grains of α iron were introduced and only one hydrated iron oxide mineral (limonite) was formed. Opal, the glassy silicate mineral, was absent. Both calcite and aragonite were positively identified in sediments from this zone, aragonite being a high-pressure transformation of calcite. All of the minerals in the host sediment were found in this zone

DISCUSSION

The pressure effects within 2 mm of the penetrator's skin were recorded in the soil by the occurrence of aragonite. Aragonite is a high-pressure phase of calcite (CaCO_3). At temperatures below 100°C , calcite can be transformed into aragonite at 4.2 kbars (ref. 7). Even though forces acting on the individual mineral grains during penetration may be predominately shearing, as evidenced by the mixed layer with crushed grains, the temperature and pressure for the calcite-aragonite transformation are not changed. Although the reaction rate is increased by these shearing forces, they do not affect the stability range for this transformation (ref. 8).

The temperature effects near the penetrator's skin ($< 1\text{ mm}$) were recorded by both the formation of new minerals and the destruction of original minerals. The destruction of clay minerals was demonstrated by the absence of particulate material in the clay size range adjacent to the penetrator's skin (fig. 10). Also, bulk chemical analyses showed that Na migration occurred. This migration feature (see table 3), where the Na content was reduced in the glassy matrix yet significantly increased in the 1–2-mm layer when compared with the host sediments, is also consistent with the destruction of clay minerals. Although the clay minerals kaolinite, illite, and montmorillonite were originally identified in the McCook sediments, none was identified in the glassy matrix next to the penetrator's skin. X-ray diffraction studies (fig. 16) on these three clay minerals at progressively higher temperature levels show the following: (a) At 300°C , most of the montmorillonite (15-Å peak) collapses to 10 Å, producing a corresponding increase in the illite peak (10-Å peak). (b) At 500°C , the remaining montmorillonite peak completely collapses and increases the illite peak even more. (c) At 700°C , the kaolinite (7-Å peak) collapses but the illite peak is unaffected. (d) At 1000°C , all clay peaks collapse, and traces of new minerals formed from the destroyed clay minerals are common (i.e., quartz, cristobolite, tridymite) in a sintered and glassy matrix. Even when material next to the penetrator's skin was concentrated, there was no evidence of any of the three clay minerals (see fig. 16, penetrators 2–5). Destruction of these clay minerals occurred in the sediments from both the full-scale and small-scale penetrators. When the X-ray diffraction studies of the clay minerals, subjected to progressively higher temperatures, from the undisturbed sediments are compared with similar studies on material from the penetrators, the results suggest the temperature experienced by the latter material was 1000°C or more. This temperature is also consistent with the Ca depletion observed in sediments adjacent to penetrators 4 and 5, assuming calcite was dissociated. Calcite dissociates, forming CaO and CO_2 at about 1000°C and 3.4 kbars (ref. 9). Finally, shard-shaped metal particles (10–100 μm in size) containing varying amounts of Cr, Fe, Ni, and Mo were common in the 0–1-mm sediment layer. None of these particles were identified as magnetite from X-ray diffraction patterns. To form a magnetite phase from the α iron phase of the original penetrator alloy, a liquid iron oxide phase

would have had to occur. The absence of a liquid oxide phase demonstrates that the temperature on the skin did not reach 1400° C (ref. 10).

In an attempt to reconstruct the sequence of events, it seems that metallic particles were abraded from the penetrator as it forced its way through the sediments. During this action, the sediments became deformed and were crushed. The skin of the penetrator became very hot and micrometer-sized metal fragments abraded. As the vehicle traveled through the soil, the heat from the penetrator raised the temperature of the soil grains in a layer about 40- μ m thick (now crushed into powder) to high temperatures, oxidized most of the micrometer-sized abraded Fe particles, and melted the clay particles of the host sediment. Cristobalite was formed upon cooling in the presence of water, during which time an opaline silica glass was formed. Small grains ($< 10 \mu$ m in size) of the lechatelierite were also formed within the glass layer. It seems likely that the iron and iron oxide fragments abraded from the penetrator's skin, and then were hydrated by the high water content in the soil. This migrating water also increased the Fe content in the matrix of the sediments that were more than 2 mm away from the penetrator's skin. The limit of mechanical mixing for the abraded iron alloy may occur where the concentration of Cr, Ni, and Mo reaches the background level in the host sediments (i.e., ~ 2 mm).

CONCLUSIONS

Field observations combined with laboratory analyses have demonstrated that mineralogical and elemental changes are produced in the sediments next to the penetrator. Contaminants introduced by the penetrator commonly occur as far away from the penetrator's skin as 2 mm (see table 6). Although volatile elements do migrate and new minerals are formed as the host minerals are destroyed in the sediment, no changes were observed beyond this 2-mm boundary. Finally, the analyses indicate that 0.58-scale penetrators could be used to simulate full-scale testing because no differences from full-scale penetrators were found in the soil modification effects.

These results indicate that either a sample retrieval mechanism or a passive ramp and entrapment device on the penetrator's exterior is essential to collect unmodified soils for the geochemistry and water-detection experiments.

Ames Research Center
National Aeronautics and Space Administration
Moffett Field, Calif. 94035, March 7, 1977

REFERENCES

1. Blanchard, M., Oberbeck, V.; Bunch, T., Reynolds, R., Canning, T., and Jackson, R.: FY1976 Progress Report on a Feasibility Study Evaluating the Use of Surface Penetrators for Planetary Exploration. NASA TM X-73,181, 1976, p. 280.
2. Blanchard, M.; and Shade, H.: The Effect of a Planetary Surface Penetrator on the Soil Column Surrounding the Impacting Body. NASA TM X-62,428, 1975.
3. Shade, H.: Preliminary Analysis of Soil Modification Found after 0.58 Scaled Penetrator Impaction on August 4, 1975, at Sandia. L.F.E. Contractor Rept. TLW 6142A, 1975.
4. Shade, H., and Polkowski, G.: Analysis of Core Samples Obtained from the McCook, Nebraska, Penetrator Test Site. L.F.E. Contractor Rept. TLW 6148B, 1976.
5. Polkowski, G. Procedures for Preserving Subsurface Fabric and Textures in Soil Adjacent to an Impacted Planetary Penetrator. L.F.E. Contractor Rept. TLW 6149, 1976.
6. Bowen, N. L.; and Auroousseau, M.. Fusion of Sedimentary Rocks in Drill-Holes. Bull Geol. Soc. Amer., vol. 34, 1923, pp. 431-448
7. Crawford, W. A., and Fyfe, W S.: Calcite-Aragonite Equilibrium at 100° C. Science, vol. 144, 1964, pp. 1569-1570.
8. Dachille, F., and Roy, R.: High-Pressure Phase Transformations in Laboratory Mechanical Mixers and Mortars. Nature, vol. 186, 1960, pp. 34-35.
9. Harker, R. J.; and Tuttle, O. F. Studies in the System CaO-MgO-CO₂ Pt. I, The Thermal Dissociation of Calcite, Dolomite, and Magnesite, American J Sci., vol. 253, 1955, pp. 209-224.
10. Darken, L. S.; and Gurry, R. W.. Physical Chemistry of Metals. McGraw-Hill Book Co., New York, 1953, pp. 350-359.

TABLE 1.— PENETRATION DEPTH AND SOIL MOISTURE AT TEST SITE,
McCOOK, NEBRASKA, JANUARY 1976

Recovery sequence	Penetrator type (D6AC steel alloy)	Impact velocity, m/sec	Depth of penetration, m	Soil moisture (% dry weight) before encasement at McCook	Soil moisture (% dry weight) after recovery at Denver
2	0.58-scale, air gun fired	159	1.83	16.1	16.8
3	Full-scale, aircraft dropped	120	2.26	15.3	14.6
4	Full-scale, aircraft dropped	133	7.93	15.3	15.4
5	0.58-scale, air gun fired	136	4.27	16.1	14.4
Soil	Saturated		3–15 cm deep	23.5	
Soil	Saturated		30 cm deep	22.1	

TABLE 2.— ELEMENTAL COMPOSITION OF PENETRATOR D6AC STEEL ALLOY

Elements	D6A-C specifications	Electron microprobe analyses (weight %) of penetrator interior
Fe	96.52–94.95	96.2
C	.45– .50	
Si	.15– .30	.2
P	.00– .10	.08
S	.00– .10	
V	.08– .15	.08
Cr	.90– 1.20	1.0
Mn	.60– .90	.7
Ni	.40– .70	.6
Mo	.90– 1.10	1.0
		<hr/> 99.86

TABLE 3.— COMPARISON OF ELEMENTAL COMPOSITION BETWEEN UNDISTURBED AND MODIFIED LOESS SEDIMENT ADJACENT TO PENETRATOR 4, McCOOK, NEBRASKA, JANUARY 1976

Element	Undisturbed soil	Soil adjacent to penetrator		
		1–2-mm zone	0–1-mm zone	Surface of glassy material
Na	0.77	1.14	1.03	0.03– 0.52
Mg	.92	.87	.70	
Al	6.23	6.28	5.66	.6 – 6.6
Si	32.11	32.55	28.62	2.4 –25.7
P	.06	.05	.04	
K	2.23	2.20	1.96	.05– 1.0
Ca	2.40	2.28	1.96	.8 – 6.2
Ti	.33	.31	.31	
Cr	34 ppm	32 ppm	359 ppm	.2 –12.5
Mn	.04	.04	.04	
Fe	2.22	2 25	7 80	14.2 –49.0
Ni	12 ppm	26 ppm	197 ppm	.02– .17
Mo	<20 ppm	<20 ppm	689 ppm	02– 7.4

TABLE 4.— COMPARISON OF ELEMENTAL COMPOSITION BETWEEN UNDISTURBED AND MODIFIED
SEDIMENT ADJACENT TO PENETRATORS 2, 3, AND 5

Element	Penetrator 2		Penetrator 3		Penetrator 5	
	Undisturbed soil	Modified soil (0–1-mm) glassy zone	Undisturbed soil	Modified soil (0–1-mm) glassy zone	Undisturbed soil	Modified soil (0–1-mm) glassy zone
Na	1.46	1.08	1.37	0.52	1.09	0.47
Mg	.51	.55	.58	.57	.84	.54
Al	6.11	5.26	6.21	5.67	6.20	4.78
Si	32.74	28.10	32.51	28.64	31.52	24.04
P	.05	.04	.05	.04	.05	.04
K	2.22	1.86	2.15	1.90	2.16	1.60
Ca	1.29	2.00	1.12	1.28	2.49	2.25
Ti	.32	.28	.32	.3	.34	.26
Cr	24 ppm	463 ppm	28 ppm	264 ppm	27 ppm	759 ppm
Mn	.07	.08	.05	.05	.04	.09
Fe	2.20	9.07	2.18	5.79	2.33	15.02
Ni	21 ppm	344 ppm	20 ppm	165 ppm	15 ppm	516 ppm
Mo	<20 ppm	844 ppm	<20 ppm	549 ppm	<20 ppm	1,440 ppm

TABLE 5.— COMPARISON OF MINERALOGICAL COMPOSITION BETWEEN
UNDISTURBED AND MODIFIED SEDIMENTS ADJACENT TO
PENETRATORS, McCOOK, NEBRASKA, JANUARY 1976

Mineral	Undisturbed soil	Soil adjacent to penetrator		
		1—2-mm zone	0—1-mm zone	Within glassy material
Silicates:				
Quartz	H	H	H	L
K-feldspar	L	L	L	L
Plagioclase	M	M	M	L
Hornblende	t	t	t	
Augite	t	t	t	
Mica	L	L	t	
Clay	L	L	t	
Opal			L	H
Cristobalite				t
Lechatelierite				t(?)
Carbonates:				
Calcite	L	L	t(?)	
Aragonite		L		
Metal:				
Iron alloy (α iron)		L	L	L
Cu-Sn alloy				t
Metal oxides:				
Ilmenite	t	t	t	
Rutile	t	t	t	
Magnetite	t	t	t	t
Limonite	t	L	L	L
Goethite			L	L
Lepidocrocite			L	t
$\epsilon\text{Fe}_2\text{O}_3$			L	
Hematite			L	L

Key: H = high
M = moderate
L = low
t = trace

TABLE 6.— SUMMARY OF CHANGES IN SEDIMENTS AT PENETRATOR IMPACT SITES
McCOOK, NEBRASKA, JANUARY 1976

Region	Material	Elemental changes		Mineralogical changes	
		Increase	Decrease	Introduced or newly formed	Depleted
0–50 μm	Glassy layer surrounding penetrator	Fe, Cr, Mo, Ni, Ca(?) (i.e., Fe 14–49%)	Si, Al, K, Na (i.e., Si 2–26%)	αFe (Fe, Cr, Mo) Magnetite (Fe_3O_4) Cu-Sn alloy Low cristobalite (SiO_2) Opal ($\text{SiO}_2 \cdot n\text{H}_2\text{O}$)	Clay Calcite Mica
50 μm –1 mm	Crushed sediment	Fe, Cr, Mo, Ni, Na	Si, Al, Ca(?)	αFe (Fe, Cr, Mo) Hematite (Fe_2O_3) Goethite ($\alpha\text{FeO} \cdot \text{OH}$) Lepidocrocite ($\gamma\text{FeO} \cdot \text{OH}$) Limonite ($\text{FeO} \cdot \text{OH} \cdot n\text{H}_2\text{O}$) $\epsilon\text{Fe}_2\text{O}_3$ Lechatelierite (SiO_2) Opal ($\text{SiO}_2 \cdot n\text{H}_2\text{O}$)	Calcite Clay
1–2 mm	Crushed sediment	Fe, Cr, Mo, Ni	None	Aragonite (CaCO_3)	Calcite

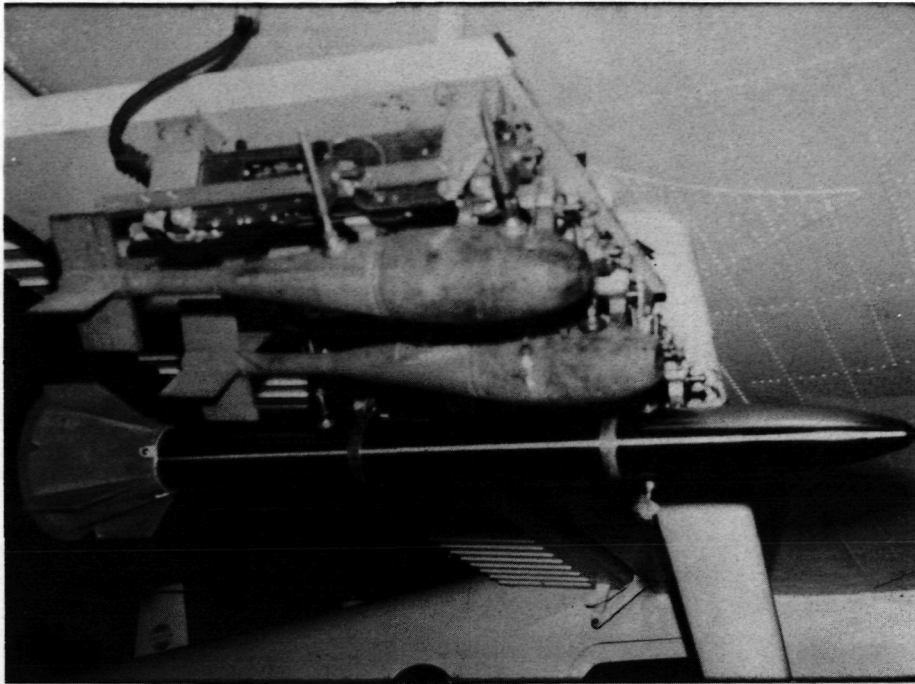


Figure 1.— Penetrator and two smoke bombs mounted under wing of aircraft before drop tests.

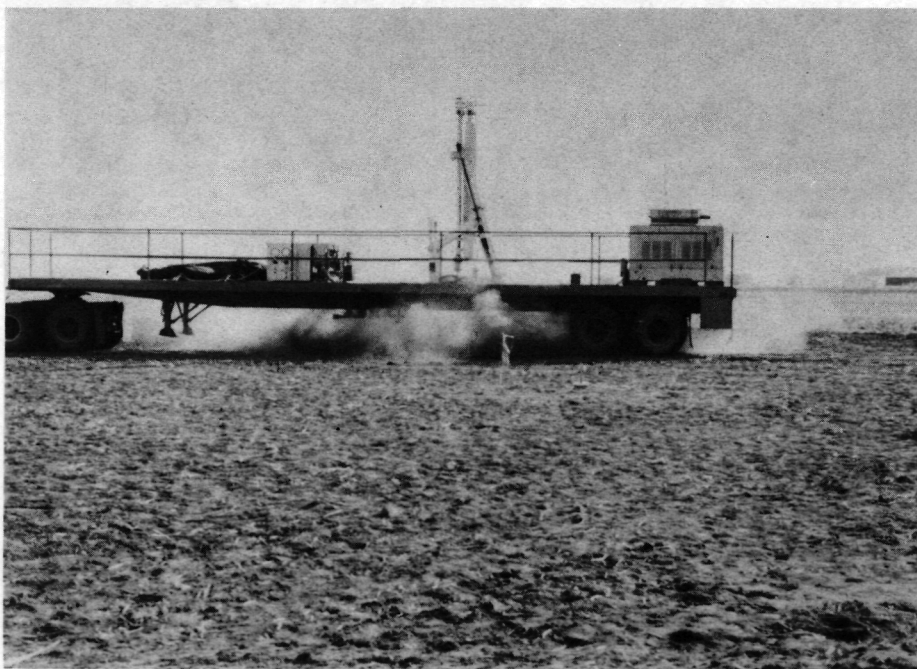


Figure 2.— Test firing from trailer-mounted air gun of 0.58-scale penetrator into layered clays and silts a few feet away from landing site of air-dropped full-scale penetrator.



Figure 3.— Air-dropped penetrator after impact into loess sediment; afterbody separated from the penetrator main body and remained at surface with antenna.



(a) Drill rig removing soil from 46-cm-diam holes inside larger 162-cm-diam hole.



(b) Larger hole with penetrator buried along its centerline.

Figure 4.— Buried penetrator being recovered.



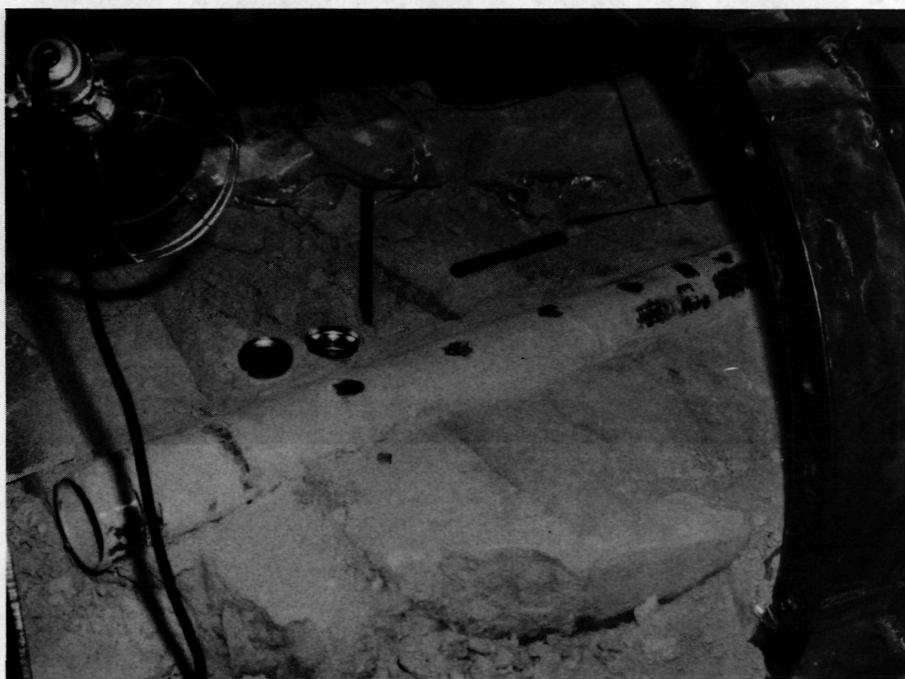
Figure 5.— Cylindrical cutting bar with jig and wall braces. When cutting bar was pushed down, cylinder of soil remained as a standing pedestal which contained the penetrator.



Figure 6.— Stainless-steel container of soil encasing penetrator.



(a) Soil samples being removed with spatula from 1-cm-thick soil layer surrounding penetrator.



(b) Metal containers used for storing millimeter thick layers of sediment adhering to the penetrator's skin.

Figure 7.— Soil samples being removed from penetrator.

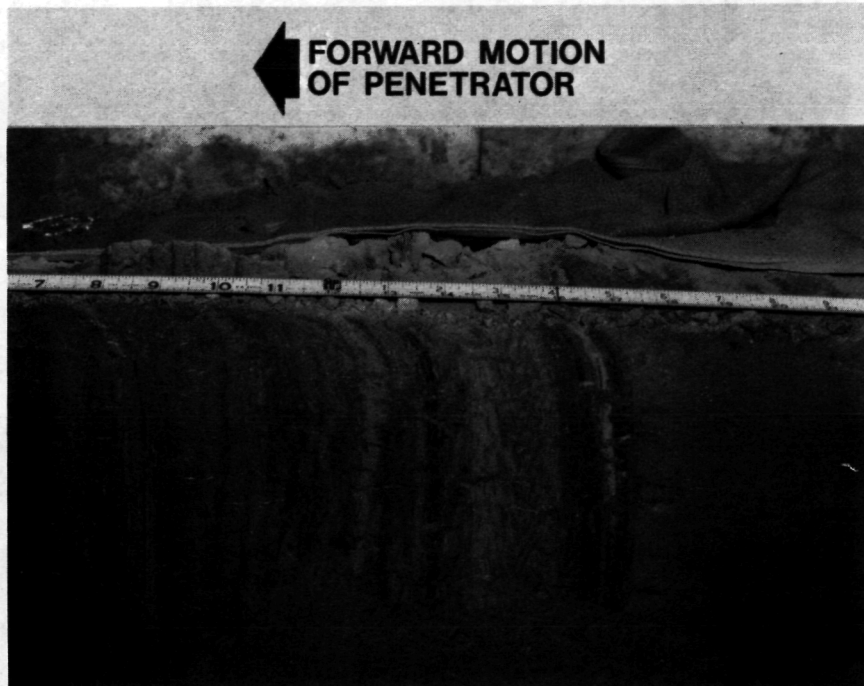
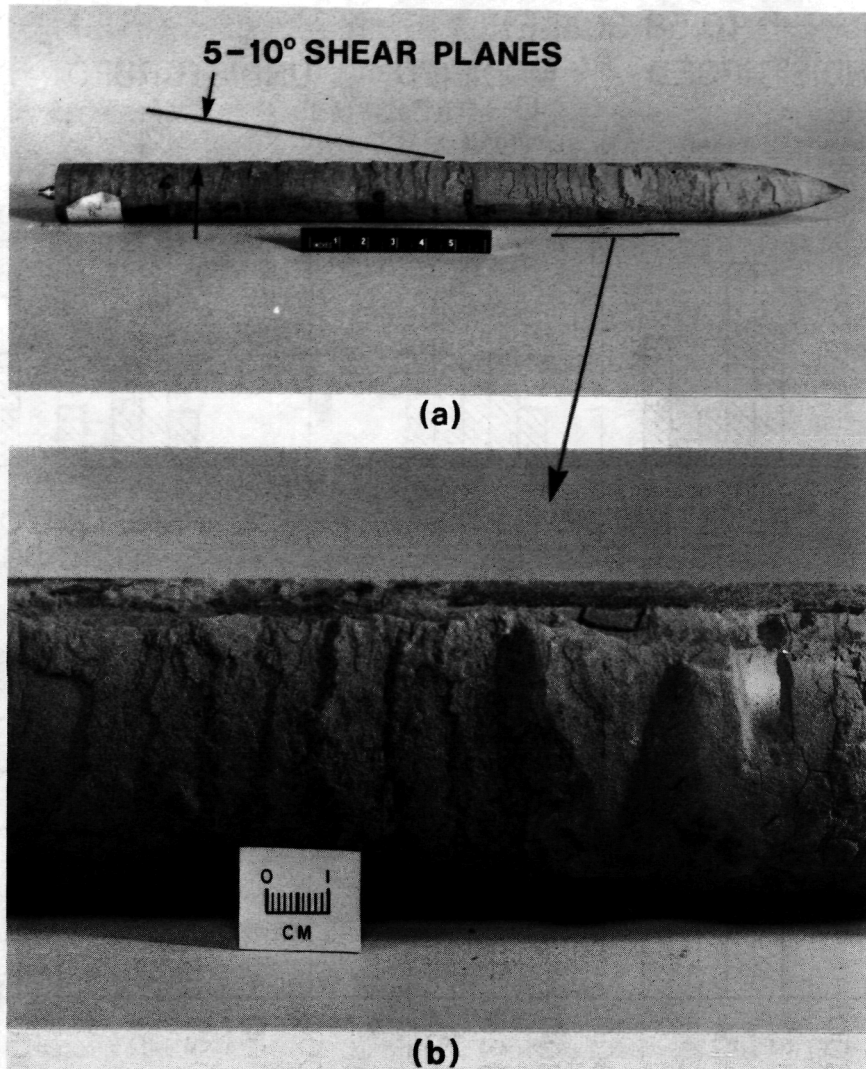


Figure 8.— Cross section of clay and silt layers at one of the penetrator impact sites; penetrator has been removed. Layers have been dragged, rotated, and thinned out in direction of forward motion of penetrator.



- (a) 0.58-scale penetrator.
(b) Closeup of shear planes.

Figure 9.— Photographs of soil (≈ 1 cm thick) adhering to penetrator showing shear planes produced during the penetrator's impact.

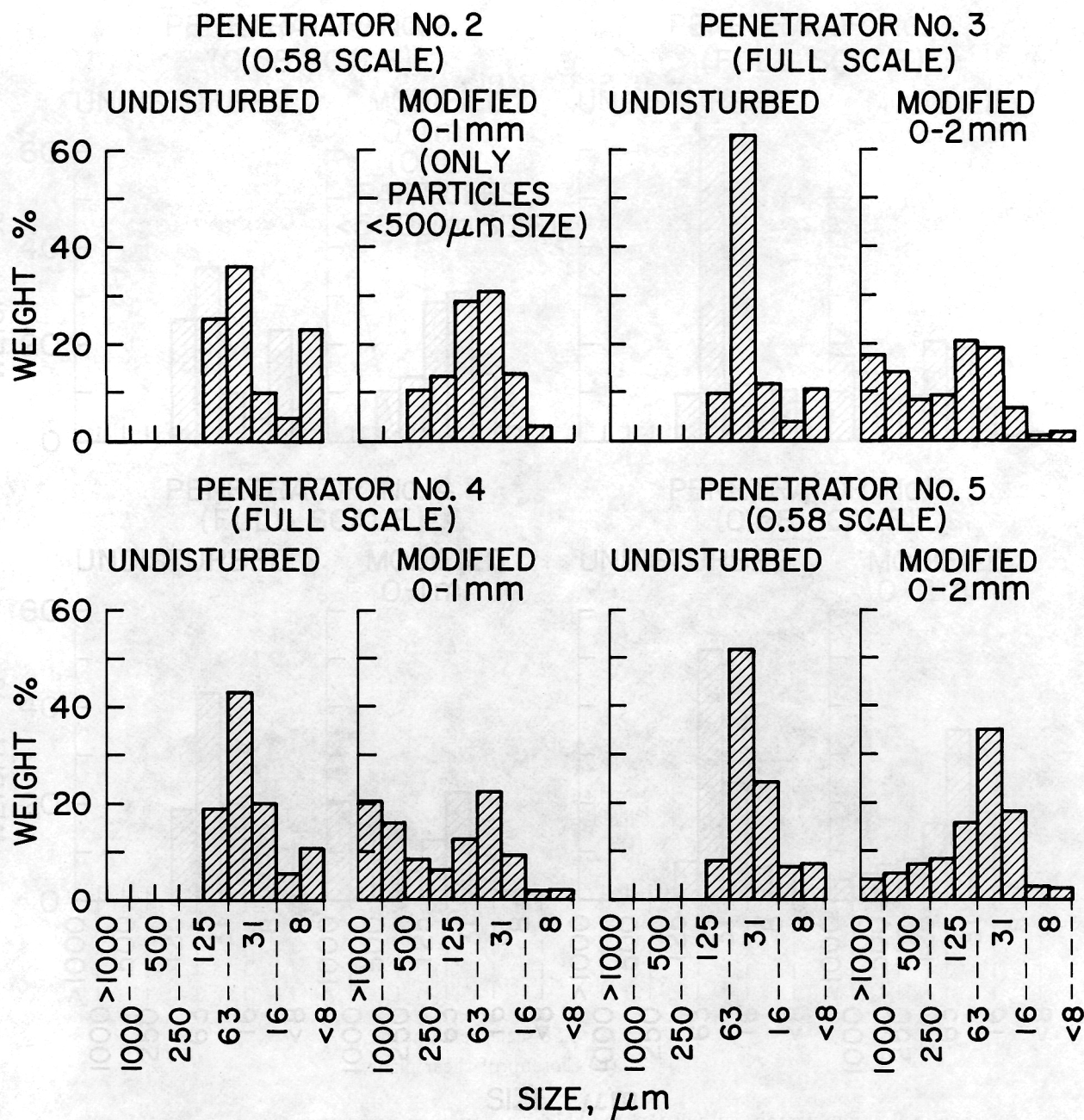
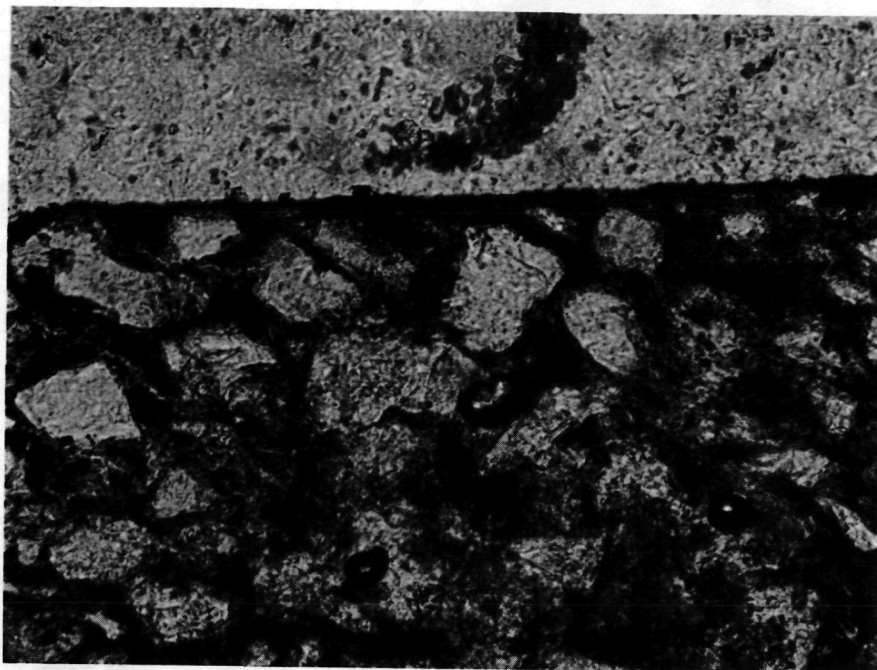
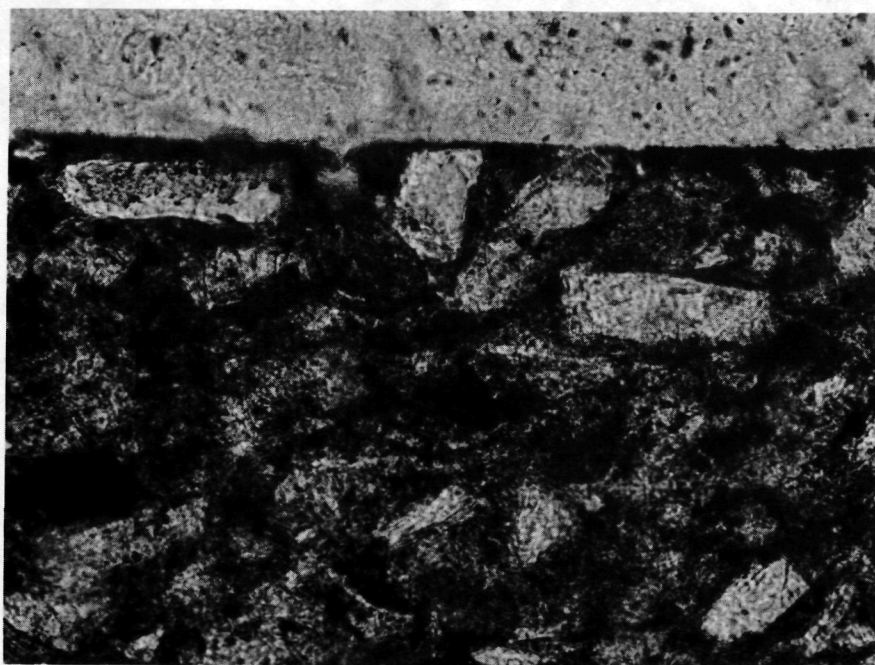


Figure 10.— Size-weight percent distribution for modified and unmodified soils at penetrator impact sites.

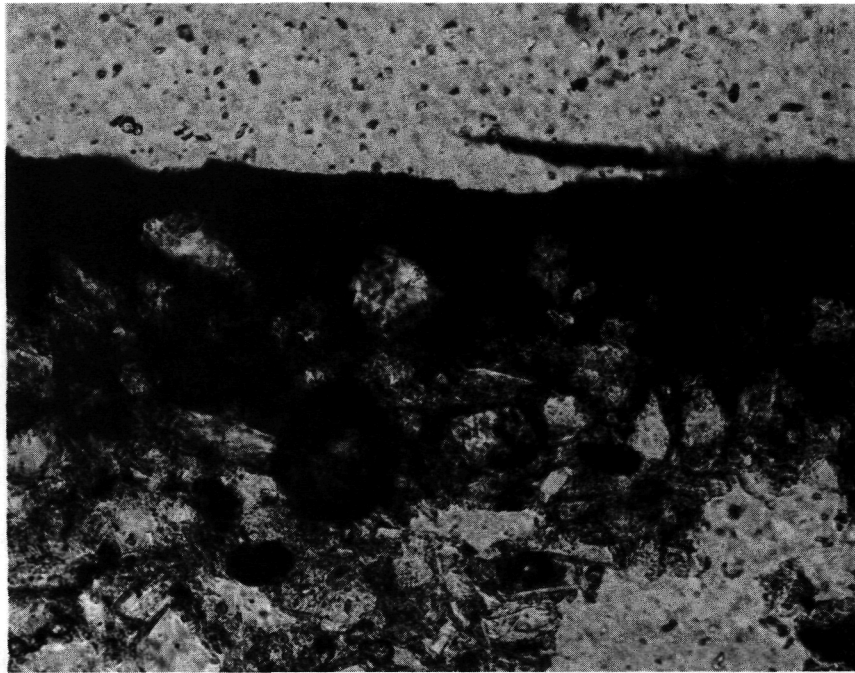


(a) Penetrator 2, 0.58 scale.

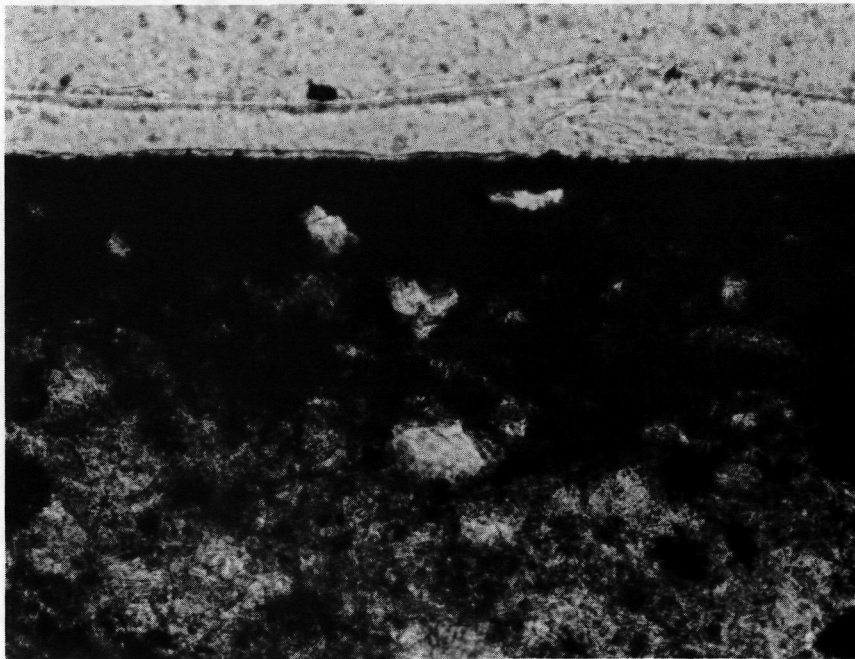


(b) Penetrator 3, full scale.

Figure 11.— Photomicrographs of petrographic thin sections of sediment adjacent to skin of each penetrator.



(c) Penetrator 4, full scale.

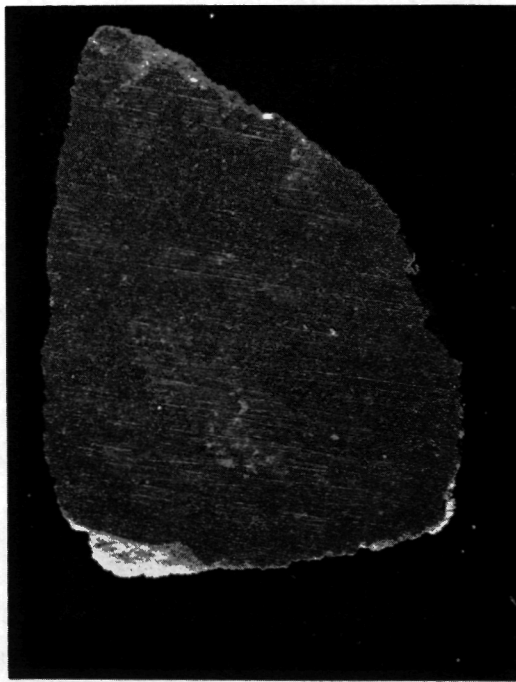


(d) Penetrator 5, 0.58 scale.

Figure 11.— Concluded.



Figure 12.— Photomicrograph of cohesive soil particles removed from the skin of penetrator 4. Soil fragment turned on edge shows soil grains cemented in glassy matrix.



(a) Photomicrograph of surface of a soil fragment facing penetrator skin with striations.



(b) Scanning electron microscope image of same fragment. Striations are casts of machine marks on skin of penetrator.

Figure 13.— Fragments of soil removed from penetrator's skin.

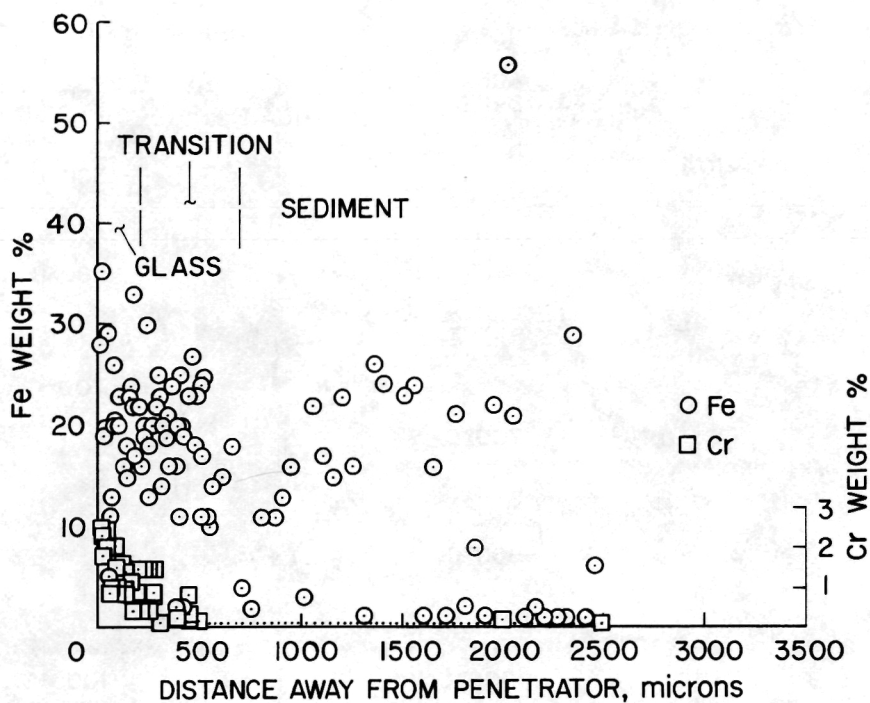


Figure 14.— Fe and Cr concentrations in glass and sediment adjacent to penetrator 4 using electron microprobe with 3- μ m spot size.

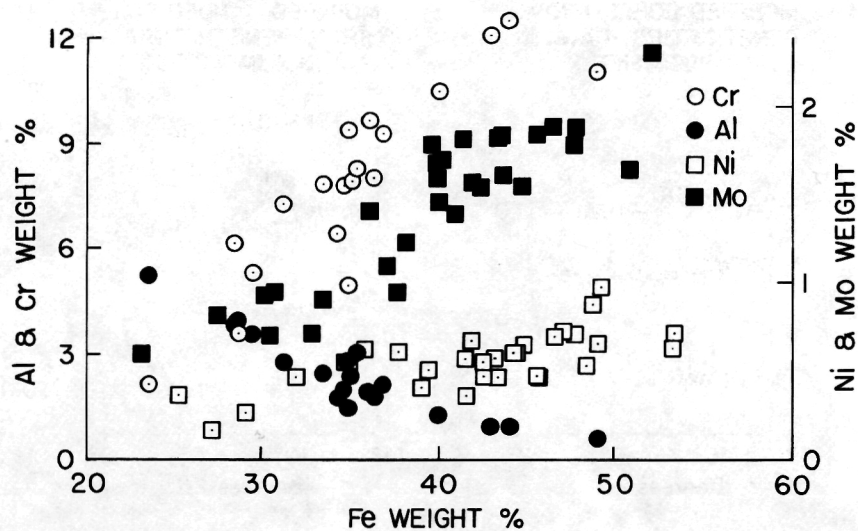


Figure 15.— Relationship between Cr, Ni, and Mo with concentration of Fe content in glassy material adjacent to penetrator 4 using electron microprobe.

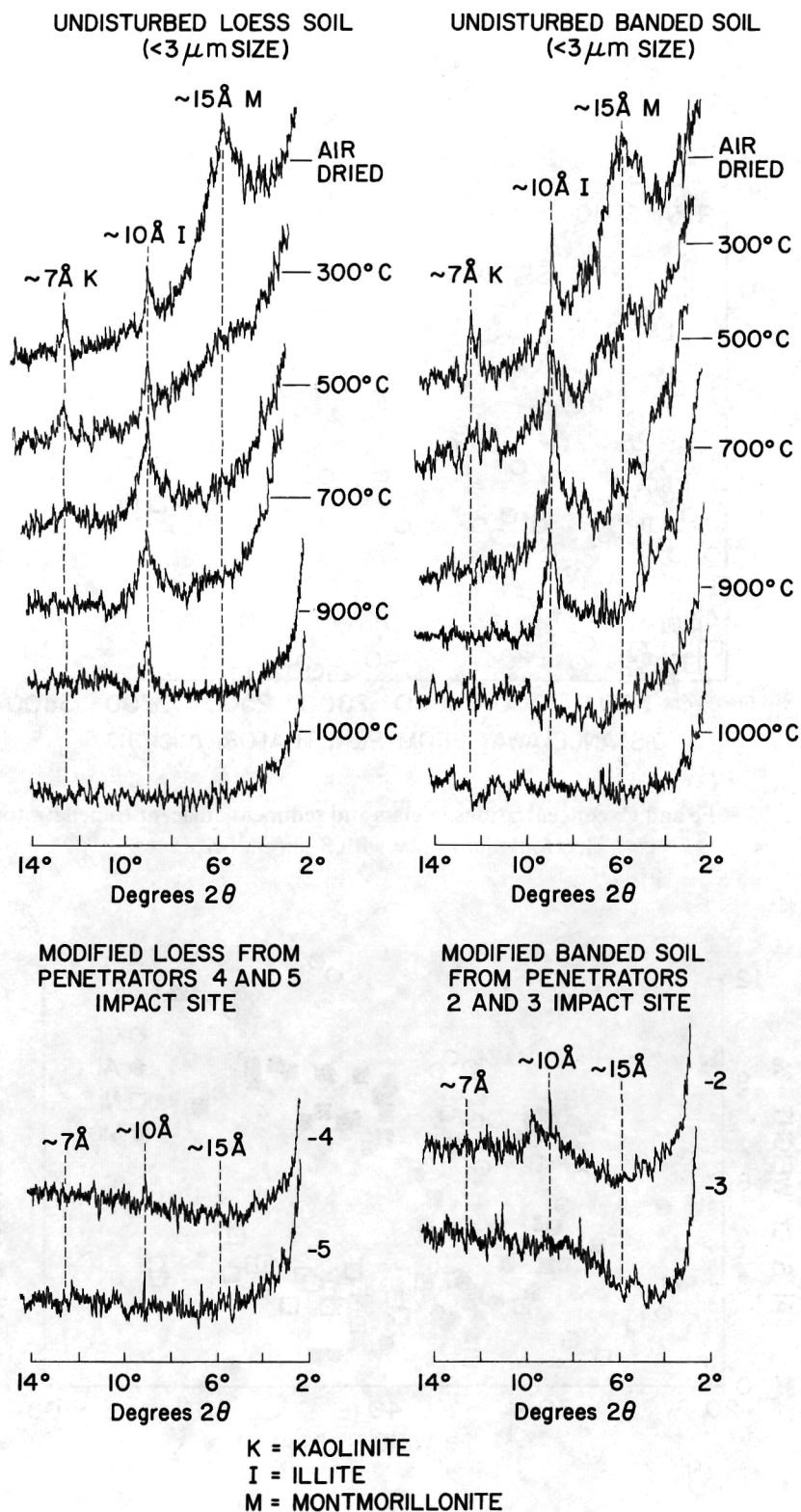


Figure 16.— Clay mineral analysis of sediments from McCook, Nebraska.



POSTMASTER: If Undeliverable (Section 158
Postal Manual) Do Not Return

"The aeronautical and space activities of the United States shall be conducted so as to contribute . . . to the expansion of human knowledge of phenomena in the atmosphere and space. The Administration shall provide for the widest practicable and appropriate dissemination of information concerning its activities and the results thereof."

—NATIONAL AERONAUTICS AND SPACE ACT OF 1958

NASA SCIENTIFIC AND TECHNICAL PUBLICATIONS

TECHNICAL REPORTS: Scientific and technical information considered important, complete, and a lasting contribution to existing knowledge.

TECHNICAL NOTES: Information less broad in scope but nevertheless of importance as a contribution to existing knowledge.

TECHNICAL MEMORANDUMS: Information receiving limited distribution because of preliminary data, security classification, or other reasons. Also includes conference proceedings with either limited or unlimited distribution.

CONTRACTOR REPORTS: Scientific and technical information generated under a NASA contract or grant and considered an important contribution to existing knowledge.

TECHNICAL TRANSLATIONS: Information published in a foreign language considered to merit NASA distribution in English.

SPECIAL PUBLICATIONS: Information derived from or of value to NASA activities. Publications include final reports of major projects, monographs, data compilations, handbooks, sourcebooks, and special bibliographies.

TECHNOLOGY UTILIZATION PUBLICATIONS: Information on technology used by NASA that may be of particular interest in commercial and other non-aerospace applications. Publications include Tech Briefs, Technology Utilization Reports and Technology Surveys.

Details on the availability of these publications may be obtained from:

SCIENTIFIC AND TECHNICAL INFORMATION OFFICE

NATIONAL AERONAUTICS AND SPACE ADMINISTRATION

Washington, D.C. 20546